

MODELED MASS AND TEMPERATURE EFFECTS OF RELEASED AND ENTRAINED SNOW ON THE LUBRICATED WET FLOW REGIME OF AVALANCHES AT BIRD HILL, SOUTHCENTRAL ALASKA

Katreen Wikstrom Jones^{1*}, Perry Bartelt² and Michael Loso³

¹ Alaska Pacific University, Anchorage, AK, USA

² WSL Institute for Snow and Avalanche Research SLF, Davos, Switzerland

³ Wrangell-St. Elias National Park, Copper Center, AK, USA

ABSTRACT: The unpredictable effects of released and entrained snow on avalanche run-out distances make hazard analysis difficult. At Bird Hill in southcentral Alaska, snow entrainment has caused small release volumes ($< 25,000 \text{ m}^3$) to develop into surprisingly far-running avalanches which endanger a highway and railroad below. In this graduate thesis project, the dynamical avalanche run-out model RAMMS was calibrated and used for the first time in southcentral Alaska. With numerical experiments on a high resolution Digital Elevation Model (DEM), produced with Structure-from-Motion photogrammetry, we examined how mass and temperature of released and entrained snow affected the lubricated wet flow regime and run-out distances. We found that temperature of the released and entrained snow was more critical than mass in determining the flow regime. Meltwater production was the predominant contributing factor to long run-out distances due to reduced basal friction as the avalanche makes the transition from the fluidized to the lubricated flow regime. The temperature of the entrained snow was most important when the entrained mass was large relative to the release mass. Warm ($\geq -1^\circ\text{C}$) entrained snow in the path made very small -3°C releases warm up quickly and become lubricated. With colder ($\leq -3^\circ\text{C}$) snow, such releases remained cold throughout the flow and stopped quickly. Monitoring of warming snow cover temperatures in the path is therefore critical for predicting flow regime transitions. The results of this project also showed that terrain features can strongly influence avalanche flow, and that detailed DEMs are therefore important, especially during shallow snow conditions.

KEYWORDS: snow entrainment, snow temperature, avalanche run-out, flow regimes, fluidization, lubrication

1. INTRODUCTION

Run-out distance is a key measure of avalanche danger in the transportation industry and is used to justify road closures. Predicting avalanche run-out distances, however, is highly problematic in an operational environment. The primary challenges are to make accurate predictions of the release mass and judge how entrainment processes will effect avalanche motion.

Despite many recent advances in the modeling of snow avalanches, the problem of snow entrainment is largely unresolved. For example, entrainment can be considered a process which will hinder avalanche motion (the avalanches “drown” in the snow cover) or entrainment can be considered a process enhancing avalanche run-out (avalanches that run on bare ground often “starve” before stopping). Under-

standing the role of entrainment on run-out remains a fundamental problem.

Early investigators defined snow entrainment as the process by which an avalanche erodes the snow cover in the path and intermixes the snow into its core (Pudasaini and Hutter, 2007). Various entrainment mechanisms were defined such as ploughing, erosion or layer fracture (Gauer and Issler, 2004). Each was associated with a different snow intake rate (Sovilla et al., 2007). The entrained snow feeds the avalanche and can contribute to significant avalanche mass growth. These investigations of snow entrainment concentrated primarily on the overall mass balance of a particular avalanche event, see for example Sovilla et al., 2007.

More recent research efforts have demonstrated the significant role of temperature (Vera Valero et al., 2015; Dreier et al., 2014; Steinkogler et al., 2014). The influx of mass is also a source of thermal energy to the avalanche core (Vera Valero et al., 2015; Naaim et al., 2013). This source evidently controls the avalanche flow temperature and therefore the avalanche flow regime (dry or wet) (Vera Valero et al., 2015). Because

* Corresponding author contact:

Katreen Wikstrom Jones

tel: +1907-268-8051

email: kwikstromjones@gmail.com

entrainment enhances shearing at the base of the avalanche, it also contributes to fluidization of the avalanche core (Vera Valero et al., 2016).

Numerical solutions have developed in order to cope with the challenge of conducting field investigations of snow entrainment in dangerous and inaccessible avalanche terrain. By adopting a numerical modeling approach we can test avalanche flow behavior under various initial release and snow cover conditions that can help us predict the variability of run-out distances.

In this model-based study, the 2-D dynamical avalanche run-out model RAMMS was implemented to examine how changes in mass and temperature of released and entrained snow influenced avalanche flow and run-out distances at Bird Hill. At this study site located between Anchorage and Girdwood in southcentral Alaska snow entrainment has caused small release volumes ($< 25,000 \text{ m}^3$) to develop into surprisingly large, fast and far-running avalanches which have endangered the Seward Highway and the Alaska Railroad that are located at the terminus of the slopes (Fig. 1) (Hamre, 2013; Murphy, 2013. Personal communication). A total of 332 avalanches were simulated with various combinations of released and entrained snow depths and temperatures in one of Bird Hill's avalanche paths. The methodology consisted of a model calibration phase (4.1) followed by a phase of numerical experiments (4.2). The results showed that meltwater production was the predominant contributing factor to long run-out distances due to reduced basal friction as the avalanche makes the transition from the fluidized to the lubricated flow regime. Small releases were more responsive to the snow conditions in the path than larger release volumes, as they warmed up faster and remained cooler depending on the entrained snow temperatures. Besides its theoretical contribution, this project was the first application of RAMMS in southcentral Alaska.

2. BIRD HILL, SOUTHCENTRAL ALASKA

Bird Hill has a steep, consistent slope angle with no transition zone (10°C slope angle) before the artificial narrow strip of flat land between the terminus of the slopes and the ocean. The Seward Highway and the Alaska Railroad run parallel at this narrow strip of land and cut through all the run-out zones (Fig. 1). The highway and the railroad are the only links between Anchorage and the Kenai Peninsula. Road closures could therefore both lead to costly financial consequences

and endanger people who need to travel to Anchorage for medical support (Murphy, 2014. Personal communication).

The snow climate at Bird Hill is typically maritime with strong temperature gradients from sea level up to ridge tops; precipitation often falls as rain at lower elevations and transitions into snow in the upper elevations. Bird Hill often receives much less snow than Girdwood and Alyeska Resort, located only a few miles east. For the past three abnormally warm winters (2013/2014 – 2015/2016) very little precipitation has fallen as snow in the region and Bird Hill has had bare ground in the lower elevations for the majority of the winter season.



Fig. 1: Steep terrain and minimal transition zone at Bird Hill (AKDOT&PF, 2014).

For this project, RAMMS was calibrated to the terrain of Bird Hill and avalanches were simulated with snow cover conditions typical for the high latitude maritime snow climate of southcentral Alaska. The path named #934 Whiskey (per AKDOT&PF and AKRR databases) was selected to represent Bird Hill's terrain in both phases of calibration and numerical experiments. The release area is small ($16,210 \text{ m}^2$) and consists primarily of a leeward west facing aspect that often gets wind-loaded. The path has a narrow gully which under shallow snow conditions directs avalanche flow. The slope angle of the path is on average 30° with one flatter section at $\sim 500 \text{ m}$ a s l, at the road crossings and also at the flat section below the cliff and the ocean that makes up the run-out zone.

3. AVALANCHE MODELING IN RAMMS

During an avalanche's descent towards the run-out zone, the avalanche mass is influenced by the topography of the path and the snow cover, which affect its mass balance, flow momentum and kinetic energy exchange (Vera Valero et al., 2015). In RAMMS, a system of partial differential equations are solved to obtain these field variables from release ($t=0$) to deposition for each pixel on a surface-induced plane. Avalanche flow is driven by gravity and follows xyz-coordinates defined by the input DEM (Christen et al., 2010). Here we describe how RAMMS incorporates snow entrainment and modifies avalanche flow behavior as a result of temperature changes in the avalanche core, the development of flow regimes, and how topography and friction play critical roles in the energy balance.

3.1 Avalanche core temperature, snow entrainment and meltwater production

The avalanche core contains kinetic energy (the slope-parallel speed of the avalanche), random energy of fluctuating snow granules R (the granular temperature), and thermal energy E (heat) (Bartelt et al., 2014). A phase change occurs when there is sufficient heat energy in the core for its temperature to exceed 0°C . In this case, meltwater is produced by dissipative heating (Vera Valero et al., 2015).

The released mass defines the initial amount of heat energy in the avalanche. This is defined by the temperature and density of the release mass. After release, the two major sources for heat energy are friction and the snow cover, that is, the temperature and density of the entrained snow (Fischer et al., 2012). Frictional shearing is not only the source of heat but also non-directional random energy R (Vera Valero et al., 2015). This is kinetic energy associated with random particle movements. It is important to note that all R that is produced in the avalanche core eventually dissipate to heat energy due to inelastic granule interactions (Vera Valero et al., 2015). Frictional shear work depends on the roughness of the terrain and on the avalanche velocity. Therefore there is great variability in the amount of heat and random kinetic energy in the avalanche.

In RAMMS, snow entrainment occurs at a rate $\dot{Q}_{\Sigma \rightarrow \phi}$ ($\text{kg m}^{-2} \text{s}^{-1}$). The model user defines the characteristics of the entrained snow, either overall or for specific sections of the path and defines the snow layer depth (m), snow temperature ($^\circ\text{C}$) and snow density (kg/m^3). The entrainment rate is

controlled by the density ratio of the snow layer and the avalanche, the slope-parallel velocity of the avalanche u_ϕ and the parameterizing erodibility parameter κ (unit less), the latter also to be defined by the model user (Christen et al., 2010):

$$\dot{Q}_{\Sigma \rightarrow \phi} = \frac{\rho_\Sigma}{\rho_\phi} \kappa u_\phi \quad (1)$$

The amount of heat influx from the entrained snow to the avalanche core (of height h_ϕ) is defined as:

$$\dot{E}_{\Sigma \rightarrow \phi} h_\phi = c_\Sigma \dot{Q}_{\Sigma \rightarrow \phi} T_\Sigma \quad (2)$$

and includes the specific heat capacity of the co-volume c_Σ , i.e. the volume of solid mass, the rate by which the snow cover is entrained $\dot{Q}_{\Sigma \rightarrow \phi}$ and the snow cover temperature T_Σ (Vera Valero et al., 2015).

3.2 Avalanche flow regimes

The two general flow regimes are fluidization and lubrication. Which one of these regimes that develops depends on the avalanche core temperature. Frictional shear work in the core \dot{W}_ϕ (and during entrainment) produces both thermal heat energy E and non-directional random energy R (J/m^2). The energy distribution drives the development of the lubricated and fluidized regimes; if most of the frictional shear work dissipates to heat, the lubricated regime is supported, and if most energy goes to R , the fluidized regime is supported.

The amount of R defines the magnitude of fluidization and depends on terrain roughness and influx of cold, low density snow. Due to inelastic granular interactions, R will dissipate to heat (Buser and Bartelt, 2009). The counteractive decay rate of R , β , depends on the warming of the avalanche core. As warm snow granules mold together, the decay rate increases which will cease the fluidized regime (Vera Valero et al., 2015).

The lubricated regime develops in warm and wet avalanches once meltwater percolates to the base. It is highly viscous and associated with high decay rates of fluctuation energy due to the molding of warm snow granules, creating a laminar flow structure with few inter-granular interactions (Vera Valero et al., 2015). Water acts as a lubricant and significantly reduces basal friction, transforming the avalanche to a plug flow gliding over the ground (Colbeck, 1992). The amount of produced meltwater describes the magnitude of lubrication and depends on influx of warm snow and dissipated heat from frictional shear work.

In avalanche paths with strong elevational snow temperature gradients it is common for multiple flow regimes to develop within one avalanche.

Commonly the fluidized regime develops first in the upper elevations from the cold released snow and as the avalanche entrains warmer snow in the lower elevations it transitions into the lubricated regime. Also in paths of significant drop height, heat dissipation from frictional shear work in the upper elevations may sufficiently warm up the avalanche core for the avalanche to transition into lubrication, independent of entrained snow temperatures in the lower elevations (Wikstroem Jones et al., 2014).

3.3 Frictional resistance

The DEM that is used as terrain input in RAMMS defines the topography of the avalanche path and the specific pixel resolution defines the terrain roughness by representing the smoothing effect of the snow cover depth (Buhler et al., 2012). RAMMS calculates the frictional resistance with a version of the Voellmy-Salm shear resistance: $\vec{S}_\phi = (S_{x\phi} S_{y\phi})$. Static friction μ controls the run-out of the avalanche by defining the slope angle at which the avalanche will begin to decelerate, and turbulent friction ξ (ms^{-2}) controls the end speed of the avalanche and makes it come to a stop. The Voellmy model is general in that μ and ξ can be assigned to reconstruct any avalanche event. In the RAMMS version 2.6.12, the Voellmy-Salm frictional resistance has been extended as follows:

$$\vec{S}_\phi = \frac{\vec{u}_\phi}{\|\vec{u}_\phi\|} \left[\mu(R)[N + F + D] + \rho_g g \frac{\|\vec{u}_\phi\|^2}{\xi_{(RKE)}} \right] \quad (3)$$

where \vec{u}_0 is avalanche velocity, R is the amount of fluctuation energy in the core, the total pressure consists of the self-weight N , forces arising from centripetal accelerations F and dispersive pressure D built up at the basal boundary from particle interactions, and ρ_g is avalanche density, and g is gravitational acceleration (Bartelt et al., 2014).

Once the avalanche core exceeds 0°C and starts to produce meltwater, RAMMS automatically assigns the static friction μ a significantly reduced value. The reduced value of μ represents the gliding of the lubricated regime to take place in the model and is a function of the meltwater content (Vera Valero et al., 2015).

4. METHODOLOGY

The methodology of this project consisted of two phases: model calibration (4.1) and numerical experiments (4.2).

4.1 Model calibration

The purpose of the model calibration was to assign values to the RAMMS input parameters that were not tested for in the numerical experiments, i.e. not the released and entrained snow depth and temperature parameters. The model calibration consisted of a sensitivity analysis of model parameters, construction of a high-resolution DEM and reconstruction in RAMMS of three historical avalanches from the path Whiskey at Bird Hill.

By calculating each model parameter's elasticity (Morris and Doak, 2002) in the sensitivity analysis it was determined which model parameters that had increasing effects on the output (Saltelli and Annoni, 2010) run-out distance and impact pressure. Among the tested model parameters, the friction parameters static friction μ , turbulent friction ξ , and the flow regime parameters production rate of $R\alpha$, and activation energy RO showed to have large effects on run-out distance and impact pressure, and were therefore to be assigned values in the avalanche reconstructions.

The DEM resolution is important in complex alpine terrain where small terrain features may affect avalanche flow and where the snow cover depth has a smoothing effect (Bühler et al., 2011). By applying the Structure-from-Motion (SfM) photogrammetry technique, a high resolution DEM of Whiskey was produced to demonstrate the typical shallow snow cover conditions at Bird Hill and use as terrain input in RAMMS. 276 photos with extensive (2/3) overlap and from oblique angles using a GPS-enabled camera were collected from a helicopter in the summer. The photos were georeferenced using ground-truth GPS points from various terrain features across the slope and the ridgeline. The DEM was built in "Photoscan Pro" version 1.0.4 by Agisoft, a software that applies a "multi-view stereo" triangulation routine to generate a 3-D view of each scene (Gauthier et al, 2014). The final DEM of 0.25 m pixel size was resampled to 2 m in ArcMAP to represent a shallow snow cover depth.

Using the 2 m DEM, three historical avalanches from Whiskey were reconstructed in RAMMS using estimated release and path conditions based on historical weather and snowpack records, and documented run-out distance and debris volume measurements. Based on the results of the reconstructed avalanches, values for the friction and flow regime parameters were assigned, and to be used as constant values in the next phase of experimental avalanche scenarios (4.2).

4.2 Numerical experiments

In the phase of numerical experiments, the effects of various mass and temperatures of released and entrained snow on avalanche flow regimes were examined by simulating avalanches and changing a release or entrained snow characteristic one-at-a-time, meaning that the following simulation had either a released or entrained snow depth changed, or a released or entrained snow temperature changed from the previous simulation.

The release volumes were defined by three released snow depths over Whiskey's typical release area (Fig. 2). Two snow entrainment zones were defined: a high zone above 500 m a s l and a low zone below 500 m a s l (Fig. 2). A total of 332 avalanches were simulated using the variations of released and entrained snow depths and temperatures listed in Fig. 3.

The maximum run-out distance for each simulation was normalized by calculating its "Beta Point ratio". This method allows for comparison of different run-outs independent to the terrain of the avalanche path (Hamre, 2014. Personal communication). The distance from the end point of the starting zone to the Beta Point (slope angle 10°) was measured. To get a normalized run-out distance as percentage to the Beta Point, for each simulation output the distance to the maximum point of run-out was divided by the distance to the Beta point. The results of the simulated avalanches were categorized based on their Beta point ratio: Category 1 being avalanches with a

maximum run-out distance percentage positive to the Beta point, and Category 2 with run-out distance negative to the Beta point.

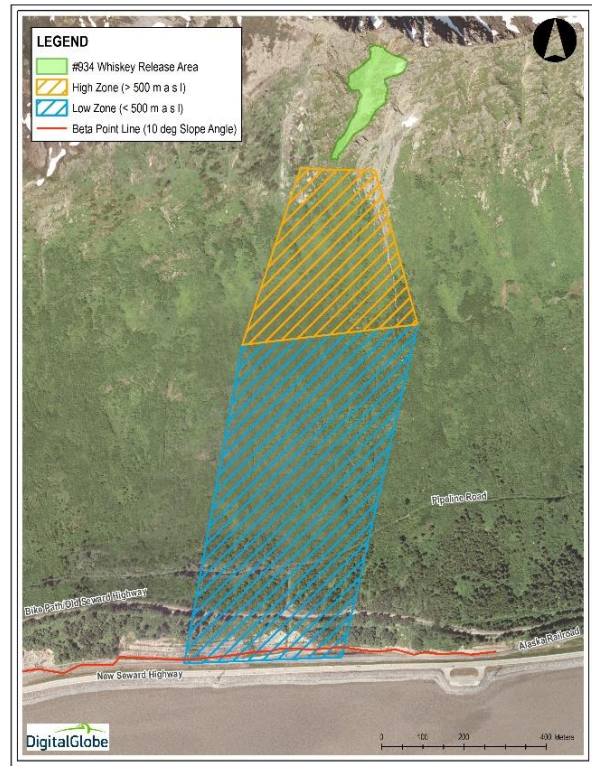


Fig. 2: Release area, entrainment zones and Beta point line (10° slope angle) for Whiskey.

	Depth	Temperature (density)	Comment
Released snow	<input type="checkbox"/> 2 m	<input type="checkbox"/> -8°C (200 kg/m ³)	* Simulated with and without 5% water content
	<input type="checkbox"/> 1 m	<input type="checkbox"/> -5°C (250 kg/m ³)	
	<input type="checkbox"/> 0.5 m	<input type="checkbox"/> -3°C (300 kg/m ³)	
		<input type="checkbox"/> 0°C (400 kg/m ³)*	
High zone	<input type="checkbox"/> 1 m*	<input type="checkbox"/> -5°C (250 kg/m ³)**	* For 2 m and 1 m release depth ** For release temp. -8°C and -5°C *** Not for release temp. 0°C **** Not for release temp. -8°C
	<input type="checkbox"/> 0.5 m	<input type="checkbox"/> -3°C (300 kg/m ³ ***)	
	<input type="checkbox"/> 0.25 m	<input type="checkbox"/> -1°C (350 kg/m ³ ****)	
		<input type="checkbox"/> 0°C (400 kg/m ³ ****)	
Low zone	<input type="checkbox"/> 1 m*	<input type="checkbox"/> -5°C (250 kg/m ³)**	* For 2 m and 1 m release depth ** For release temp. -8°C and -5°C *** Not for release temp. 0°C
	<input type="checkbox"/> 0.5 m	<input type="checkbox"/> -3°C (300 kg/m ³ ***)	
	<input type="checkbox"/> 0.25 m	<input type="checkbox"/> -1°C (350 kg/m ³ ****)	
	<input type="checkbox"/> 0 m	<input type="checkbox"/> 0°C (400 kg/m ³)	

Fig. 3: Tested input parameter values in numerical experiments.

5. RESULTS

The results of the numerical experiments showed that the released snow temperature had the strongest correlation with run-out distance closely followed by the snow temperature in the high zone (Fig. 4). This was demonstrated by the 49% of simulated avalanches that became Category 1 avalanches where meltwater production generated their long run-out distances. An early onset and increase in the amount of meltwater lead to increased run-out distances, explaining why all 0°C releases became Category 1 avalanches and that this number decreased with colder released snow temperatures. For the colder releases of -8°C and -5°C, only avalanches that entrained -1°C snow or warmer in the high zone obtained long run-out distances.

The development of the fluidized and lubricated flow regimes were demonstrated by the maximum amount of meltwater produced, maximum avalanche core temperature, and maximum average random energy R (Fig. 5). The results clearly showed that meltwater was the predominant contributor to long run-out distances by enabling the transition into the lubricated flow regime. As expected, meltwater was produced in all

Category 1 avalanches with a minimum amount of 5 mm/m² for respective flow height (Fig. 5).

How fast the avalanche core warmed up primarily depended on mass influx of warm snow in the high zone, and in cases when the core was

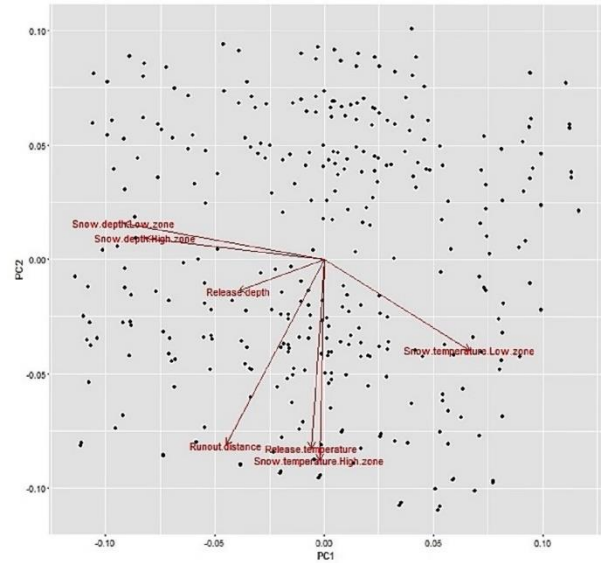


Fig. 4: Similar length and direction of vectors indicate similar meaning in the context of the data of tested input variables and run-out distance for the first (PC1) and second (PC2) principal components.

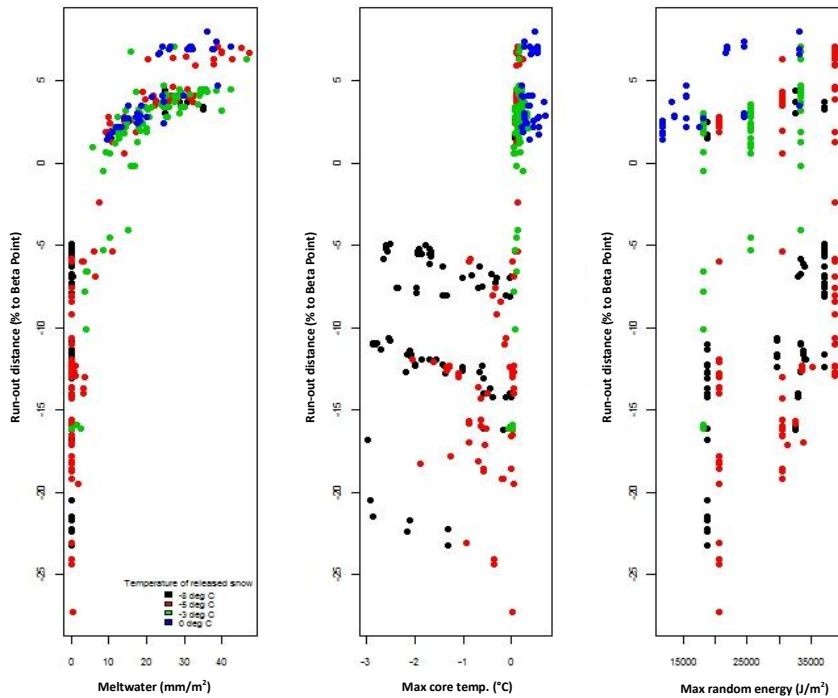


Fig. 5: Flow regime variables and run-out distance. (Left) Maximum amount of meltwater (mm/m²) and run-out distance, (center) maximum avalanche core temperature (°C) and run-out distance, and (right) maximum random energy (J/m²) and run-out distance.

close to 0°C, it depended on snow temperatures in the low zone. Some of the colder avalanches reached 0°C but did not produce enough meltwater to become lubricated (Fig. 5). Increased snow temperature in the low zone from -3°C to -1°C and foremost from -1°C to 0°C enabled these cold avalanches to enhance meltwater production and transition into lubrication (Fig. 6). In scenarios with bare ground in the low zone, early onset of lubrication caused by warm snow temperature in the high zone was required for avalanches to glide over the rough terrain and generate long run-out distances.

The amount and duration of produced R in the high zone, proportionally dissipated to heat, appeared critical in determining the warming of the avalanche core temperature, in particular for medium warm releases (-3°C) that entrained consistently cold (-3°C) snow in the path (Fig. 6). Because the amount of produced R was smaller in the smallest releases (release volume < 8,000 m³) i.e. less dissipated heat, they remained cool by

entraining cold snow at lower elevations while the larger amounts of dissipated heat in the larger releases enabled for quick warm up despite continued entrainment of cold snow in the low zone.

Local observations indicate that large and cold releases often resist the effects of lubrication and carry a highly fluidized core far into the wet snowpack of the lower elevations (Hamre, 2016. Personal communication). The numerical results agreed and showed that avalanche size mattered for how efficiently the entrained snow could alter the current flow regime. The results showed that a small, cold avalanche release was more responsive to variations in entrained snow depths and temperatures in the path than larger cold releases.

6. CONCLUSIONS

We adopted a numerical modeling approach by implementing RAMMS under an experimental design to examine the effects of mass and

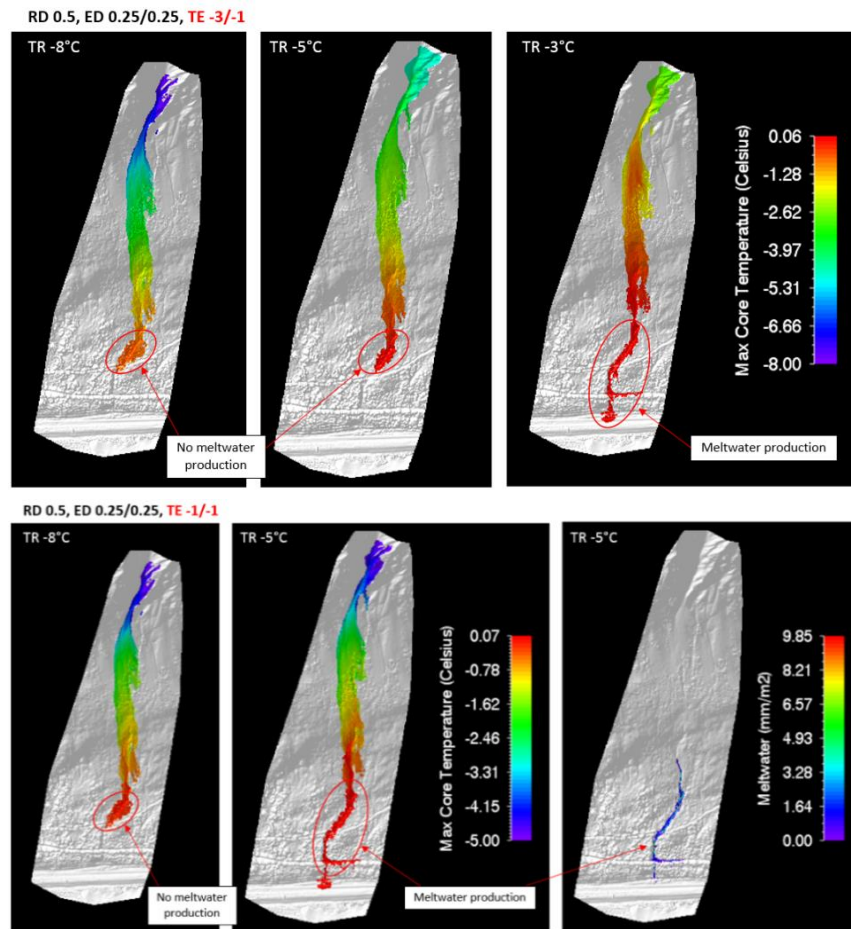


Fig. 6: Effects of increased released snow temperature on maximum avalanche core temperatures in 0.5 m releases with snow depth 0.25 m in the high and low zone, and (top row) snow temperature -3°C in the high zone and -1°C in the low zone; (bottom row) snow temperature -1°C in the high and low zone.

temperature of released and entrained snow on avalanche flow regime. We found that:

- Temperature of released and entrained snow was more critical than mass in determining flow regime, with a close correlation between meltwater production and long run-out distances with the flow regime transition from fluidization into lubrication.
- The temperature of the entrained snow was most important when the entrained mass was large relative to the release mass. Warm ($\geq -1^{\circ}\text{C}$) entrained snow in the path made very small -3°C releases warm up quickly and become lubricated. Colder ($< -1^{\circ}\text{C}$) entrained snow made these small medium warm releases remain cold throughout the flow and starve early.
- Larger sized releases were able to produce meltwater due to influx of dissipated heat from random kinetic energy produced in the upper elevations which enabled them to warm up and become lubricated despite cold entrained snow in the lower elevations.

Based on these results, we suggest for more accurate run-out distance predictions, detailed mapping of the path's terrain features, and close monitoring of snow temperatures during weather events that could rapidly warm up the snow, e.g. rain or strong solar radiation in the spring.

The numerical experiments in this project were designed to trigger an avalanche's transition from the fluidized to the lubricated regime as it reached the lower elevations and entrained warmer snow. All simulated avalanches were constrained by the "Wet snow" *R* regime in RAMMS and inability to form a powder cloud. Continued work in this region will be focused on examining powder avalanche flow using various DEM resolutions and implementing the "Mixed powder" *R* regime in RAMMS.

ACKNOWLEDGEMENTS

We would like to thank Dave Hamre at AKRR, Matt Murphy and Timothy Glassett at AKDOT&PF, Jim Kennedy (Alyeska Resort), Eeva Latosuo at Alaska Pacific University, and Cesar Vera Valero at SLF. Thank you to AKRR, SLF, Cora Shea Memorial Fund and American Alpine Club for financial support of the project.

REFERENCES

- Bartelt, P., Buser, O., Bühler, Y., L. Dreier, L., Christen, M., 2014. Numerical simulation of snow avalanches: Modelling dilatative processes with cohesion in rapid granular shear flows. *Numerical Methods in Geotechnical Engineering – Hicks, Brinkgreve & Rohe (Eds)*, Taylor & Francis Group, 327-332
- Buser, O., Bartelt, P., 2009. Production and decay of random kinetic energy in granular snow avalanches. *J. Glaciol.* 55, 189
- Bühler, Y., Christen, M., Kowalski, J., Bartelt, P., 2011. Sensitivity of snow avalanche simulation to digital elevation model quality and resolution. *Ann. Glaciol.* 52, 58, 72-80
- Colbeck, S. C., 1992. A review of the processes that control snow friction. *CRREL Monogr.* 92-2
- Christen, M., Kowalski, J., Bartelt, P., 2010. RAMMS: Numerical simulation of dense snow avalanches in three-dimensional terrain. *Cold Reg. Sci. Technol.* 63, 1-2, 1 – 14
- Dreier, L., Bühler, Y., Steinkogler, W., Feistl, T., Bartelt, P., 2014. Modelling small and frequent avalanches. *Proceedings of the International Snow Science Workshop*. Banff, Canada
- Fischer, J-T., Kowalski, J., Pudasaini, S. P., 2012. Topographic curvature effects in applied avalanche modelling. *Cold Reg. Sci. Technol.* 74-75, 21-30
- Gauthier, D., Conlan, M., Jamieson, B., 2014. Photogrammetry of fracture lines and avalanche terrain: Potential applications to research and hazard mitigation projects. *Proceedings for International Snow Science Workshop*, Banff, 2014
- Mears, A., 1989. Regional Comparisons of avalanche-profile and runout data. *Arct. Alp. Res.*, 3, 283-287
- Morris, W. F., Doak, D. F., 2002. *Quantitative Conservation Biology: Theory and Practice of Population Viability Analysis*. 1st Ed. Sinauer Associates
- Naaim, M., Durand, Y., Eckert, N., Chambon, G., 2013. Dense avalanche friction coefficients: influence of physical properties of snow. *J. Glaciol.* 59, 216, 771-782
- Pudasaini, S. P., Hutter, K., 2007. *Avalanche Dynamics. Dynamics of Rapid Flows of Dense Granular Avalanches*, Springer, 602
- Saltelli, A., Annoni, P., 2010. How to avoid a perfunctory sensitivity analysis. *Env. Mod. Softw.*, 25, 1508-1517
- Sovilla, B., Margreth, S., Bartelt, P., 2007. On snow entrainment in avalanche dynamics calculations. *Cold Reg. Sci. Technol.* 47, 69-79
- Steinkogler, W., Sovilla, B., Lehning, M., 2014. Influence of snow cover properties on avalanche dynamics. *Cold Reg. Sci. Technol.* 97, 121-131
- Vera Valero, C., Wikstroem Jones, K., Bühler, Y., Bartelt, P., 2015. Release temperature, snow-cover entrainment and the thermal flow regime of snow avalanches. *J. Glaciol.* 61, 225
- Wikstroem Jones, K., Hamre, D., Bartelt, P., 2014. Effects of the thermal characteristics of snow entrainment in avalanche run-out at Bird Hill, South-central Alaska. *Proceedings of the International Snow Science Workshop*. Banff, Canada